

UCLA
COMPUTATIONAL AND APPLIED MATHEMATICS

Level Set Methods for the Simulation of Epitaxial Phenomena

Mark F. Gyure
Christian Ratsch
Barry Merriman
Russel E. Caflisch
Stanley Osher
Jennifer J. Zinck
Dimitri D. Vvedensky

March 1999

CAM Report 99-11

Department of Mathematics
University of California, Los Angeles
Los Angeles, CA. 90095-1555

Level set methods for the simulation of epitaxial phenomena

Mark F. Gyure,¹ Christian Ratsch,^{1,2} Barry Merriman,² Russel E. Caflisch,² Stanley Osher,² Jennifer J. Zinck,¹ and Dimitri D. Vvedensky^{1,2*}

⁽¹⁾ *HRL Laboratories LLC, 3011 Malibu Canyon Road, Malibu, CA 90265*

⁽²⁾ *Department of Mathematics, University of California, Los Angeles, CA 90095-1555*

(October 9, 1998)

We introduce a model for epitaxial phenomena based on the motion of island boundaries, which is described by the level set method. Our model treats the growing film as a continuum in the lateral direction, but retains atomistic discreteness in the growth direction. An example of such an “island dynamics” model using the level set method is presented and compared with the corresponding rate equation description. Extensions of our methodology to more general settings are then discussed.

PACS: 02.30.Jr, 68.35.Fx, 81.10.Aj, 02.40.Ey

Modeling epitaxial growth presents an enormous challenge to theoretical physicists and materials scientists. The range of length and time scales represented by problems of practical interest (e.g., the growth of device layers) spans many orders of magnitude [1], i.e., atomistic processes can significantly affect quantities such as surface morphology even at the largest length and time scales [2]. A complete model for epitaxial growth would seamlessly combine the submonolayer and multilayer regimes on lateral scales of several microns or more, be appropriate for a variety of homoepitaxial and heteroepitaxial systems, and be capable of describing different growth techniques.

None of the models for epitaxial growth currently in use can accomplish this objective. The most common approaches fall into one of two categories: analytic-based methods, i.e. homogeneous rate equations and continuum equations of motion, and kinetic Monte Carlo (KMC) simulations. Homogeneous rate equations are straightforward to formulate [3], but do not readily yield information on surface morphology. Moreover, the number of parameters required grows quickly once rate equations are extended to the coalescence or multilayer growth regimes [4]. Even in the pre-coalescence regime, the physical interpretation and computation of these parameters in terms of atomistic processes are often unclear at best, unattainable at worst.

Continuum equations of motion that take the form of partial differential equations [5] for the surface height profile do yield information on morphology at large length scales. As they are typically formulated [5,6], however, continuum equations are appropriate only in a regime where the surface is already assumed to be macroscopically rough. Continuum methods are therefore unsuitable for describing atomic scale roughness. The primary advantage of these and rate equation methods is the vast methodology available for, e.g., identifying asymptotic regimes (scaling) [7] and performing stability analyses [8].

KMC simulations [9] offer an alternative to analytic approaches. They allow easy implementation of a wide

range of atomistic kinetic processes, which can in principle be identified and their rates determined from first principles calculations [10]. However, simulations are usually based on the length and time scales of single atoms and adatom hopping rates, so modeling systems of practical interest is not always feasible. In addition, due to the stochastic nature of simulations, the advantages of analytic approaches mentioned above are not readily obtained.

Yet, despite the practical limitations of analytic and simulational methods, they have been used with great effect to provide a comprehensive conceptual and computational framework for describing homoepitaxial growth [11], especially by molecular-beam epitaxy. Problems arise, however, when attempts are made to extend these techniques to heteroepitaxial systems, where the effects of lattice mismatch must be incorporated, or to other growth methods, such as vapor-phase epitaxy (VPE), which requires coupling the atomistic kinetics on the substrate to the hydrodynamic delivery of new material. Some aspects of these issues have been addressed for particular systems, but no general methodology has emerged to provide a unifying framework in the spirit of the analytic or simulational work described above.

In this paper, we introduce a new model and closely-related numerical technique that addresses these issues. In our model, growth is described by the creation and subsequent motion of island boundaries; hence, we refer to this model as “island dynamics.” The model is discrete in the growth direction, but continuous in the lateral directions and therefore, in principle, can describe growth on arbitrarily large lateral length scales. Moreover, since the lateral directions are treated continuously, continuum equations representing any field variable can be coupled to the growth by solving the appropriate boundary-value problem for the field and using local values of this field to determine the local velocity of the island boundaries. For example, the strain fields that occur in the presence of lattice mismatch or the hydrodynamic fields in a VPE reactor can be accommodated by this method.

Although island dynamics is a natural way of describ-

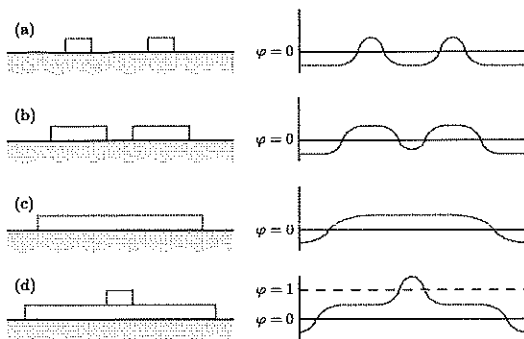


FIG. 1. Schematic evolution of one-dimensional island morphologies (left) and the corresponding level set function, φ (right): (a) two spatially separated islands, (b) the same islands at a later time, but before coalescence, (c) the islands after coalescence, and (d) the nucleation of a new island on top of the coalesced islands.

ing many aspects of epitaxial growth, its implementation requires tracking a large number of individual interfaces that coalesce or are created by nucleation. Recent advances in applied mathematics, in particular, the development of the level set method for simulating the motion of free boundaries [12,13], now make numerical implementation of such a model practical. We first will give a brief introduction to the level set method and then present results of a basic island dynamics model to demonstrate its viability.

The central idea behind the level set method [12] is that any boundary curve Γ , such as a step or the boundary of an island, can be represented as the set $\varphi = 0$, called the *level set*, of a smooth function φ [Fig. 1(a)]. For a given boundary velocity \mathbf{v} , the equation for φ is then

$$\frac{\partial \varphi}{\partial t} + \mathbf{v} \cdot \nabla \varphi = 0 \quad , \quad (1)$$

in which \mathbf{v} has been extended in an arbitrary way from the boundary $\Gamma(t)$. Since $\nabla \varphi = \hat{\mathbf{n}} |\nabla \varphi|$, then $\mathbf{v} \cdot \nabla \varphi = v |\nabla \varphi|$, where $v = \hat{\mathbf{n}} \cdot \mathbf{v}$ is the normal component of \mathbf{v} and $\hat{\mathbf{n}}$ points along the direction of $\nabla \varphi$. Growth is naturally described by the smooth evolution of φ as illustrated schematically in Figs. 1(a,b). The boundary curve $\Gamma(t)$ generally has several disjoint pieces that may evolve so as to merge [Fig. 1(c)] or split [13,14].

We have extended this method to multilayer growth where the (zero thickness) boundaries $\Gamma_k(t)$ of the islands are defined as the set of spatial points \mathbf{x} for which $\varphi(\mathbf{x}, t) = k$ for $k = 0, 1, 2, \dots$ [Fig. 1(d)]. Overhangs and undercuts, generally considered irrelevant in modeling epitaxial phenomena, are prevented by using one single-valued function φ for all layers. The evolution of the level set function φ is obtained by numerically solving Eqn. (1) with high-order accuracy (typically third order) using essentially nonoscillatory (ENO) methods [15].

An important feature of the level set method is that φ remains smooth throughout coalescence. This is crucial

for applications to epitaxial growth because hundreds or even thousands of island boundaries may merge in the course of a typical simulation. While other methods for tracking boundaries (e.g. [16]) require additional input for accommodating the topological changes that occur during coalescence, the evolution of boundaries with the level set method is a direct consequence of a particular choice for the boundary velocity \mathbf{v} .

To illustrate the application of the level set method to epitaxial growth, we consider a basic island dynamics model. This model assumes that the adatom density $\rho = \rho(t)$ is spatially uniform and that the incident flux F is constant in space and time. If we also assume that adatoms attach irreversibly to the islands, then the velocity of the island boundary has magnitude

$$v = D\rho a \quad , \quad (2)$$

where D is the adatom diffusion constant and a is the lattice constant. The adatom density increases due to the flux and decreases due to both nucleation of new islands and attachment of adatoms to island boundaries. The equation for the evolution of the adatom density is thus given by

$$\frac{d\rho}{dt} = F - n_0 \frac{dN}{dt} - \frac{v}{a^2 L^2} \int ds \quad , \quad (3)$$

where n_0 is the number of adatoms in a new island, N is the density of islands, L is the system size and the integral is over all the island boundaries. The form of the last term, which accounts for the decrease of adatom density due to attachment to island boundaries, is easily understood by observing that the integral over all island boundaries with a spatially constant v is just the total area of adatoms swept up by these boundaries in time dt . The factor of a^2 then converts this area into the number of adatoms lost and the factor of L^2 converts this, in turn, into the corresponding density.

Equations (2) and (3) are closed by specifying the nucleation rate. For the case of irreversible attachment, $n_0 = 2$ and the nucleation rate is

$$\frac{dN}{dt} = D\rho^2 \quad . \quad (4)$$

New islands are nucleated at the times t_n when NL^2 crosses the integer value n . At these times a ‘‘peak’’ is inserted into φ [cf. Fig. 1(d)]. This peak is one unit high and spans several points on the numerical grid to ensure the smoothness of φ . Since there is no spatial dependence in the adatom density and, hence, in the nucleation rate, we choose the location \mathbf{x}_n of new islands to be random. This is equivalent to adding a source term $\sum_n \delta(t - t_n) \delta(\mathbf{x} - \mathbf{x}_n)$ to the right-hand side of Eq. (1). While this nucleation scheme is appropriate here, the temporal and spatial dependence of nucleation can be chosen to include any desired physics, such as the spatial variation of the adatom density.

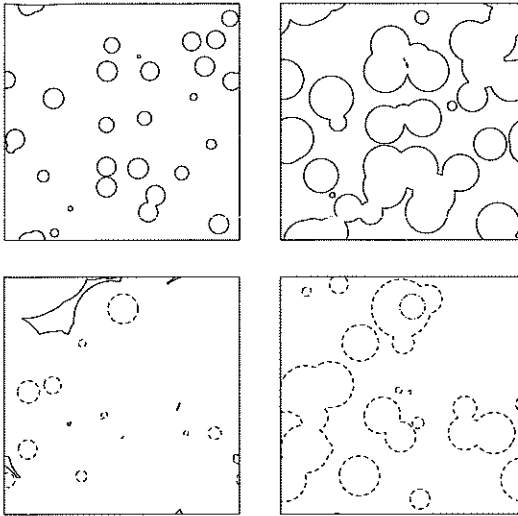


FIG. 2. Island boundaries in the first (solid), second (dashed), and third (dash-dotted) layers for the model of epitaxial growth described in the text. The coverages in monolayers (ML) are 0.1 (upper left), 0.5 (upper right), 1.0 (lower left) and 1.3 (lower right). Data were obtained for $D/F = 10^6$, $L/a = 180$, and a numerical grid of linear size 256.

The above model describes the growth of islands at a rate proportional to their perimeter, which is appropriate for the period immediately preceding the aggregation regime [17]. While no fixed island growth rates are correct for all regimes [17,18], our choice is suitable for demonstrating the feasibility of applying the level set method to a particular island dynamics model. Figure 2 shows islands at four different coverages obtained by integrating Eqns. (1), (3), and (4). Since the model is both isotropic and spatially uniform, the islands are circular, but this is not an intrinsic limitation of our method. The velocity for the island boundaries can reflect any underlying crystal symmetry [19].

This simple island dynamics model is best understood in the context of rate equations that take into account the evolution of a finite number of islands in a finite system of size L , but with continuous island sizes. Consider Eq. (3) in the slightly altered form

$$\frac{d\rho}{dt} = F - n_0 \frac{dN}{dt} - \frac{v}{a^2 L^2} \sum_i 2\pi r_i, \quad (5)$$

where we make explicit the sum over the perimeter of every island in the system whose radius is r_i . With evolution equations for each r_i given by

$$\frac{dr_i}{dt} = v, \quad (6)$$

this set of equations, together with Eqs. (2) and (4), is then formally identical to the island dynamics model prior to coalescence, provided that all $r_i = 0$ initially

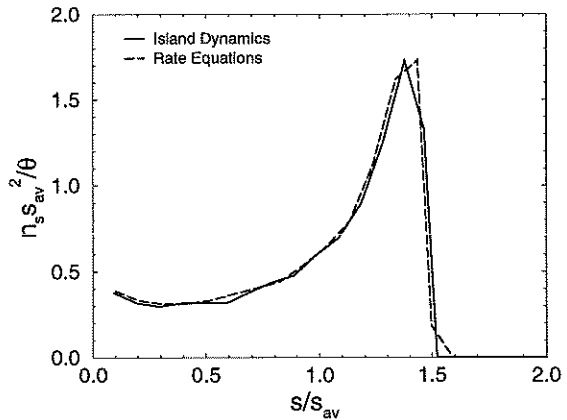


FIG. 3. Comparison of the scaled island size distributions for the island dynamics simulation and real space rate equations, where n_s is the density of islands of size s and s_{av} is the average island size. Data shown were obtained for $D/F = 10^6$ and a coverage $\theta = 0.2$ ML.

and that the k th nucleation event adds a new island to the system with initial radius $r_k = a\sqrt{n_0/\pi}$. Because the system size enters explicitly into these coupled equations, we refer to them as “real space” rate equations [20].

To provide a quantitative comparison between the island dynamics model and real space rate equations, we examine the scaled island size distributions [21] produced by the two models. Figure 3 shows the results of the island dynamics simulation and integration of the real space rate equations. All data has been obtained with $L/a = 718$; the island dynamics simulations were performed on a numerical grid of linear size 1024. These values were chosen to resolve dimers in a numerically stable way. This system size is large enough that finite size effects are negligible. To facilitate comparison with the real space rate equations, seeding is chosen to exclude coalescence. The excellent agreement in Fig. 3 confirms that the island dynamics simulation, in which island boundaries are moved by the level set function, produces quantitatively correct results for this simple model. In particular, it confirms the accuracy of the numerical evolution of the level set function.

We now turn to the interpretation of the data. The island size distributions exhibit two distinct characteristics: a rather sharp cutoff which moves to the left as D/F increases (not shown) and a long tail for smaller islands. This can be understood as follows. The island dynamics model evolves a discrete number of islands of finite size. A large number of islands is nucleated near the onset of growth which then grow to approximately the same size. This results in a peak near the largest island size followed by a sharp cutoff. Subsequently, the adatom density reaches a steady state and then, according to Eq. (4), new islands are nucleated at a constant rate. This leads to the long tail for small islands. As D/F increases, the relative number of islands nucleated at early times in-

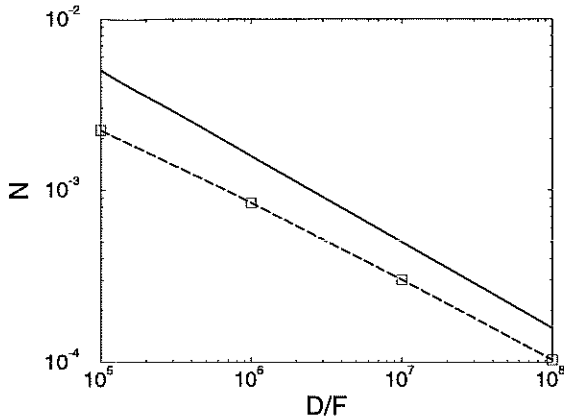


FIG. 4. Island density obtained from island dynamics simulations as a function of D/F at a coverage $\theta = 0.05$ ML. The dashed line is a guide to the eye and the solid line has slope $-1/2$.

creases at the expense of the smaller islands, leading to a shift of the peak position toward $s/s_{av} = 1$. As a result, the island density decreases and we obtain scaling behavior consistent with $N \sim (D/F)^{-1/2}$ (Fig. 4). This agrees with the standard rate equation analysis for this model [22] and KMC simulations for the pre-aggregation regime [17].

The approach we have described here has applicability far beyond the basic model we have used. The most obvious extension of our model is to solve a diffusion equation for the adatom density and use the density gradient at island edges to determine the growth velocity of island boundaries. This is currently being pursued and results will be published elsewhere. Just as in the case of adatom diffusion, values of a local strain field can be used to determine the growth velocity of island boundaries during heteroepitaxial growth. It is also possible to construct an island dynamics model for VPE, in which a hydrodynamics simulation for an entire reactor is used to provide local values of density and chemical composition at the surface of a wafer. Such a calculation was done in a similar, but simpler, framework in Ref. [14]. In conclusion, we believe that the availability of robust level set methods represents an opportunity to attack problems in epitaxial growth within a new framework.

We gratefully acknowledge support of this work by NSF and DARPA through cooperative agreement DMS-9615854 as part of the Virtual Integrated Prototyping Initiative.

* Permanent address: The Blackett Laboratory, Imperial College, London SW7 2BZ, United Kingdom.

[1] *Proceedings of the Workshop on Virtual Molecular Beam*

Epitaxy, edited by M. F. Gyure and J. J. Zinck, Comp. Mat. Sci. **6**, pp. 113-196 (1996).

- [2] A.-L. Barabasi and H. E. Stanley, *Fractal Concepts in Surface Growth* (Cambridge University Press, Cambridge, England, 1995).
- [3] J. A. Venables, G. D. T. Spiller, and M. Hanbücken, Rep. Prog. Phys. **47**, 399 (1984).
- [4] R. Kariotis and M. G. Lagally, Surf. Sci. **216**, 557 (1989).
- [5] J. Villain, J. Phys. I **1**, 19 (1991).
- [6] D. D. Vvedensky, A. Zangwill, C. N. Luse, and M. R. Wilby, Phys. Rev. E **48**, 852 (1993).
- [7] D. E. Wolf, Phys. Rev. Lett. **67**, 1783 (1991); E. Frey and U. C. Tauber, Phys. Rev. E **50**, 1024 (1994); T. Sun and M. Plischke, Phys. Rev. E **50**, 3370 (1994).
- [8] A. W. Hunt, C. Orme, D. R. M. Williams, B. G. Orr, and L. M. Sander, Europhys. Lett. **27**, 611 (1994); L. Golubović, Phys. Rev. Lett. **78**, 90 (1997).
- [9] J. D. Weeks and G. H. Gilmer, Adv. Chem. Phys. **40**, 157 (1979); S. Clarke and D. D. Vvedensky, Phys. Rev. Lett. **58**, 2235 (1987); A. Madhukar and S. V. Ghaisas, CRC Crit. Rev. Sol. State and Mater. Sci. **14**, 1 (1988); H. Metiu, Y.-T. Lu, and Z. Y. Zhang, Science **255**, 1088 (1992).
- [10] C. Ratsch, P. Ruggerone, and M. Scheffler, in *Surface Diffusion: Atomistic and Collective Processes*, edited by M. C. Tringides (Plenum, New York, 1997), pp. 83-101.
- [11] J. Y. Tsao, *Materials Fundamentals of Molecular Beam Epitaxy*, (Academic Press, Boston, 1993).
- [12] S. Osher and J. A. Sethian, J. Comp. Phys. **79**, 12 (1988).
- [13] S. Chen, B. Merriman, S. Osher, and P. Smereka, J. Comp. Phys. **135**, 8 (1997).
- [14] M. Sussman, P. Smereka, and S. Osher, J. Comp. Phys. **114**, 146 (1994); D. Peng, B. Merriman, S. Osher, H. K. Zhao, and M. Kang, unpublished.
- [15] C.-W. Shu and S. Osher, J. Comp. Phys. **83**, 32 (1989); S. Osher and C.-W. Shu, SIAM J. Num. Anal. **28**, 12 (1991).
- [16] D. Juric and G. Tryggvason, J. Comp. Phys. **123**, 127 (1996).
- [17] J. G. Amar and F. Family, Thin Solid Films **272**, 208 (1996).
- [18] M. C. Bartelt and J. W. Evans, Phys. Rev. B. **54**, R17359 (1996).
- [19] R. E. Caffisch, M. F. Gyure, B. Merriman, S. Osher, C. Ratsch, D. D. Vvedensky, and J. J. Zinck, Appl. Math. Lett. (in press).
- [20] Note that there is a fundamental conceptual difference between the real space rate equations and the conventional rate equations [3]. The real space rate equations describe the evolution of a discrete number of islands with continuous sizes seeded at discrete times. In contrast, conventional rate equations describe the evolution of a continuous number density of islands of discrete size seeded continuously in time. These differences have several manifestations which will be published elsewhere.
- [21] M. C. Bartelt and J. W. Evans, Phys. Rev. B **46**, 12675 (1992).
- [22] J. A. Blackman and A. Wilding, Europhys. Lett. **16**, 115 (1991).